EVOLUTION & DEVELOPMENT 7:4, 289–300 (2005)

Co-option of an oral–aboral patterning mechanism to control left–right differentiation: the direct-developing sea urchin *Heliocidaris erythrogramma* is sinistralized, not ventralized, by $NiCl_2$

Sharon B. Minsuk*,[1] and Rudolf A. Raff

Department of Biology and Indiana Molecular Biology Institute, Indiana University, Bloomington, IN 47405, USA

*Author for correspondence (email: sharon.minsuk@kli.ac.at)

[1]Present address: Konrad Lorenz Institute for Evolution and Cognition Research, Adolf Lorenz Gasse 2, A3422 Altenberg, Austria.

SUMMARY Larval dorsoventral (DV) and left–right (LR) axial patterning unfold progressively in sea urchin development, leading to commitment of the major embryonic regions by the gastrula stage. The direct-developing sea urchin *Heliocidaris erythrogramma* has lost oral–aboral differentiation along the DV axis but has accelerated vestibular ectoderm development on the left side. $NiCl_2$ radializes indirect-developing sea urchins by shifting cells toward a ventral fate (oral ectoderm). We treated embryos of *H. erythrogramma* and the indirect-developing *H. tuberculata* with $NiCl_2$. *H. tuberculata* was ventralized exactly like other indirect developers, establishing that basic patterning mechanisms are conserved in this genus. *H. erythrogramma* was also radialized; timing, dosage response, and some morphological features were similar to those in other sea urchins. Ectodermal explant and recombination experiments demonstrate that the effect of nickel is autonomous to the ectoderm, another feature in common with indirect developers. However, *H. erythrogramma* is distinctly sinistralized rather than ventralized, its cells shifting toward a left-side fate (vestibular ectoderm). This geometric contrast in the midst of pervasive functional similarity suggests that nickel-sensitive processes in *H. erythrogramma* axial patterning, homologous to those in indirect developers, have been redeployed, and hence co-opted, from their ancestral role in DV axis determination to a new role in LR axis determination. We discuss DV and LR axial patterning and their evolutionary transformation.

INTRODUCTION

Evolutionary transformations of axial orientation may have been important in several major macroevolutionary events, including axial reorganization at the origin of Bilateria (Finnerty et al. 2004), dorsoventral (DV) inversion during chordate evolution (Gerhart 2000), and the origin of pentamery in echinoderms (Popodi and Raff 2001). It is therefore important to understand how axial ontogeny can be altered. Here, we investigate a transformation of an axial patterning mechanism at the species level.

Axial patterning is a central question in developmental biology, and sea urchins have been a focus of this inquiry for over a century. The best understood of the three orthogonal embryonic axes is the animal–vegetal (AV) axis, stretching from the animal to the vegetal pole (reviewed in Hörstadius 1973; Brandhorst and Klein 2002; Angerer and Angerer 2003). The AV axis is specified maternally in the cytoarchitecture of the egg, which is radially symmetrical around this axis. The other two axes, the DV axis, which is manifest mainly in the differentiation of the ectoderm into the oral and aboral territories, and the left/right (LR) axis, are not specified until after fertilization in most sea urchins (Hörstadius 1973; Henry 1998; Brandhorst and Klein 2002; Angerer and Angerer 2003). (The DV axis is often called the oral/aboral axis, but we reserve the terms "oral" and "aboral" to refer to the differentiated tissues that form along that axis, and their associated gene expression territories. The tissue type is dissociable from the axis per se, as this study illustrates.) It is not known how these axes are initially specified. Once specified, pattern formation along all three axes unfolds progressively, leading to definitive commitment of the major regions of the embryo by the gastrula stage.

The direct-developing sea urchin *Heliocidaris erythrogramma* presents a number of contrasts with indirect developers. Its early cleavage divisions have been modified, and its cell lineages reorganized accordingly (Wray and Raff 1989, 1990). It has lost the distinctive larval arms, and severely reduced the elaborate larval skeleton, resulting in a simpler oblong larva. In particular, it has no trace of oral or aboral territories, or a larval mouth or anus, and its open-ended ciliated band no longer serves as a territory boundary. However, the DV axis is present and distinct (as indicated by the bilateral symmetry of the ciliated band and larval skeleton),

and homologous to that of other sea urchins (Emlet 1995; Byrne et al. 2001; Wilson et al. 2005a). (It is because this axis is homologous in all sea urchins, yet lacks any features of "oral" or "aboral" in *H. erythrogramma*, that it must be called the "dorsoventral" axis. Oral and aboral territories lie along that axis in indirect developers, but the axis can exist without them.) In contrast to the reduction of larval features, adult rudiment development on the left side is accelerated and exaggerated. A large left coelom and vestibule dominate the larval anatomy beginning at the end of gastrulation, between 20 and 30 h postfertilization. The adult rudiment develops within the vestibule and emerges at metamorphosis after as little as 3.5 days. All the unique features of this species are recently derived, within the last 4 million years (Zigler et al. 2003); the closest relative, *H. tuberculata*, undergoes standard indirect development (Raff 1987).

H. erythrogramma shares the regulative early development of other sea urchins, although in keeping with its general developmental theme, its LR axis is specified earlier, before first cleavage (Henry and Raff 1990). Like the DV and LR axes of indirect developers, this axis becomes fully committed around gastrulation (Henry et al. 1990; Henry and Raff 1994; Minsuk et al. 2005). In this study, we further investigate the patterning of the DV and LR axes.

In their description of *H. erythrogramma* larval development, Williams and Anderson (1975) described an alternative "constricted" morph of *H. erythrogramma* larvae having a circumferential ring of vestibular ectoderm in which the adult rudiment developed. It was later realized (Henry and Raff unpublished) that these specimens represent a spontaneously occurring abnormality. Based on the morphology and morphogenetic behavior of these forms, we have hypothesized that this abnormality is in fact a highly specific radialization of the larva by circumferential expansion of a left-side territory (vestibular ectoderm) at the expense of the dorsal, ventral, and right-side territory (larval or "extravestibular" ectoderm). We therefore predicted that we should be able to induce the same phenotype artificially by treatment with a reagent known to cause the radialization of sea urchin embryos, $NiCl_2$ (Rulon 1953; Lallier 1956; Timourian and Watchmaker 1972; Hardin et al. 1992). However, in indirect-developing sea urchins, $NiCl_2$ treatment causes the expansion of ventral territory (oral ectoderm), not left-side territory (Hardin et al. 1992). No ventralized phenotype has been observed in *H. erythrogramma*. This raises the question of whether the spontaneously observed radialized phenotype is in fact comparable with that observed in radialized indirect developers, and whether nickel treatment would duplicate the spontaneous phenotype or, alternatively, bring about a novel ventralized phenotype. Answers to these questions have important implications for understanding DV and LR axis formation in sea urchins, and can tell us which features of axis formation are evolutionarily labile.

We treated embryos of both *H. erythrogramma* and its indirect-developing sister species, *H. tuberculata*, with $NiCl_2$ throughout development at a range of concentrations. *H. tuberculata* responds to nickel like other indirect developers, establishing that basic patterning mechanisms are conserved in this genus. In nickel-treated *H. erythrogramma*, the spontaneously occurring phenotype is duplicated. A characterization of this effect reveals many features in common with the ventralization of indirect-developing sea urchins, including graded partial radialization effects of timing and dosage, and a sensitive period from blastula through midgastrula. Ectodermal explants and reciprocal ectoderm/archenteron recombinants between treated and untreated embryos demonstrate that the effect of nickel is autonomous to the ectoderm, also as in indirect developers. Yet, in *H. erythrogramma*, nickel distinctly causes sinistralization (a shift of tissue phenotypes at a given position along the LR axis, toward those normally found further to the left) rather than ventralization. This geometric contrast in the midst of pervasive functional similarity suggests an evolutionary redeployment of homologous nickel-sensitive processes in *H. erythrogramma* axial patterning, and provides clues about the nature of these processes and about the interaction between DV and LR patterning in sea urchins.

MATERIALS AND METHODS

Gametes of *H. erythrogramma* and *H. tuberculata* were obtained from adults injected with 0.55-M KCl. Embryos of both species were cultured at 19–25°C, in 0.45-μm Millipore-filtered sea water (FSW) containing $NiCl_2$ at various concentrations. In each *H. erythrogramma* experiment, approximately 50 embryos were cultured in a 100-mm diameter culture dish. The much smaller *H. tuberculata* embryos were cultured in larger numbers, at approximately equal density for each treatment. Embryos were treated throughout their development, beginning at the two-cell stage. Shorter treatment pulses covered portions of the first day of development, followed by transfer back into FSW with several rinses. Dead or dying *H. erythrogramma* embryos were removed from the dishes. Except where noted, results were uniform within each treatment across all surviving embryos.

Microsurgery was performed on untreated and $NiCl_2$-treated *H. erythrogramma* gastrulae as described in Minsuk and Raff (2002). Ectodermal shells were produced by the removal of archenterons (including endodermal and coelomic precursors). Reciprocal recombinants were produced by inserting $NiCl_2$-treated archenterons into untreated ectodermal shells, and vice versa. Ectodermal shells and recombinants were then cultured in FSW.

Embryos were photographed on a Zeiss stereoscope under epi-illumination, or on a Zeiss Axioplan compound microscope (Carl Zeiss, Thornwood, NY) either under bright field, or under polarized light to view the birefringent $CaCO_3$ skeleton. In many cases, embryos and larvae were lightly fixed in 2% paraformaldehyde in FSW before photographing in order to eliminate swimming. $NiCl_2$-treated larvae (alive or fixed) tended to stand vertically in the dish

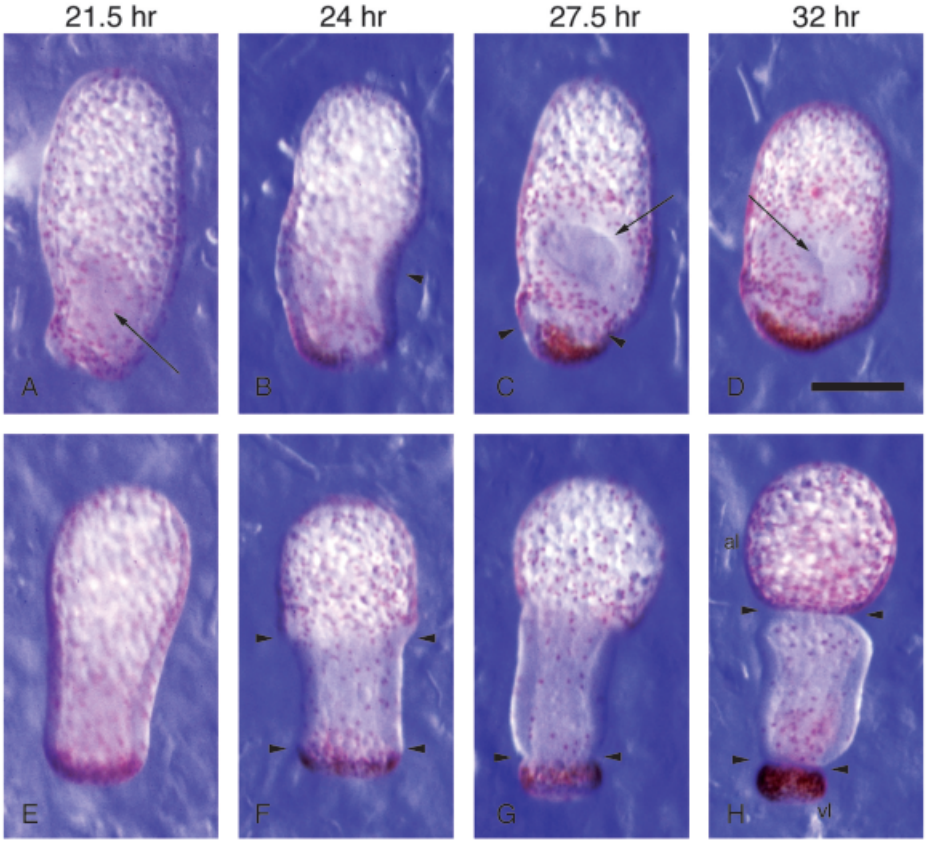

Fig. 1. Morphogenesis of untreated control (A–D) and corresponding $NiCl_2$-treated (E–H) *Heliocidaris erythrogramma* embryos immediately postgastrulation. Age increases from left to right as indicated. Animal is up, and vegetal is down in all panels. Small colorless spheres within each embryo are lipid droplets. Note gradual accumulation of red pigment cells in both control and treated embryos, especially at the vegetal pole, as development progresses. (A–D) Untreated controls, viewed from the left side (hence dorsal is to the right in photos), except B. (A) Note the large lipid-free spot (arrow). A tracing of this embryo is shown in Fig. 4. (B) (in ventral view) Note the concave left side, at right in photo (arrowhead). (C) Note the oval lip of the vestibular opening surrounding the invaginated vestibule (arrow). Pigment-free stripe near the vegetal end is the presumptive ciliated band (arrowheads). (D) Small vestibular opening (arrow) conceals incipient tube feet now present within the vestibule. (E–H) $NiCl_2$-treated embryos, radially symmetrical. (E) At the earliest departure from normal morphology, the embryo begins to take on a light bulb shape. (F) Note distinct tissue boundaries (arrowheads). (G) Note constriction pinching off larval ectoderm at the vegetal end (arrowheads). (H) Larval ectoderm is now pinched off at both ends (arrowheads). Vestibular ectoderm (central section) has taken on an hourglass shape, narrowest in the middle. al, animal lobe; vl, vegetal lobe. Bar: 200 μm.

because of the segregation of the buoyant lipid droplets to the animal pole. When viewed on the compound microscope, they were lightly squashed under a cover slip or held in a very shallow uncovered depression slide, but in order to photograph them in lateral view when viewed through the stereoscope, larvae were laid on a dense suspension of methylcellulose in FSW.

RESULTS

$NiCl_2$-treated *H. tuberculata* embryos develop into ventralized larvae after gastrulation

The response of *H. tuberculata* embryos to nickel (data not shown) was similar to that of *Lytechinus variegatus* embryos (Hardin et al. 1992), but with a greater dosage sensitivity. Treatment at 50 μM produced the ventralized phenotype described by Hardin et al. (1992) for *L. variegatus* at 500–2000 μM, including the circumferential skeletal ring (nucleated at three to five sites, compared with 10–12 in *L. variegatus*) and the same radialized morphology without larval arms or pigment cells. Embryos treated with only 5.0-μM $NiCl_2$ developed intermediate phenotypes similar to those of *L. variegatus* at 100–250 μM, with an expanded oral field, often lacking the oral hood and associated anterolateral arms but with one or two extra postoral arms, and with reduced numbers of pigment cells. Embryos treated with 500-μM $NiCl_2$ responded similarly to *L. variegatus* treated at 5000 μM, suffering severe gastrulation defects and completely lacking skeleton.

$NiCl_2$-treated *H. erythrogramma* embryos develop a radialized larval morphology surrounded by a circumferential band of vestibular ectoderm

As in *H. tuberculata*, treatment of *H. erythrogramma* embryos in a range of $NiCl_2$ concentrations resulted in a series of phenotypes from partial radialization at lower doses, through full radialization at higher doses, to additional severe defects at excessive doses.

Embryos treated with moderate doses of $NiCl_2$ (2–10 μM, in nine separate experimental runs—about 450 embryos) were indistinguishable from untreated embryos through the end of gastrulation. They cleaved and hatched normally, developed the normal uniform ciliation and swimming behavior (spinning around their AV axes), gastrulated normally, and

began the AV elongation typical of normal late- and post-gastrulae. The first signs of abnormal development occurred at the same time that untreated embryos displayed the first signs of LR asymmetry. The blastocoel of *H. erythrogramma* is filled with lipid droplets, everywhere visible through the transparent ectoderm (Williams and Anderson 1975; Henry et al. 1991). In normal embryos, the first symmetry-breaking event is the formation of the left coelom at the tip of the archenteron (Williams and Anderson 1975; Haag and Raff 1998; Ferkowicz and Raff 2001). The first external asymmetry is the appearance of a lipid-free spot in the vegetal half of the left side, where the developing left coelom presses up against the ectoderm, excluding the droplets (Fig. 1A). This is followed shortly thereafter by a thickening of the ectoderm on that side of the embryo, which later gives rise to the vestibule. In $NiCl_2$-treated embryos, small lipid-free spots arose at the same position along the AV axis but distributed around the circumference of the embryo, and that region of the embryo began to decrease in diameter. These lipid-free spots merged into a continuous circumferential band. The thickening of the ectoderm, instead of being restricted to one side, took place throughout the circumferential band, which continued to constrict, forcing the embryo to take the shape of a light bulb (Fig. 1E), pushing most of the lipid droplets up to the animal pole while a small portion remained at the vegetal pole.

Next, as the left-side ectoderm of control embryos differentiated into definitive vestibular ectoderm, becoming flattened and then concave as it began to invaginate (Fig. 1B), the circumferential band of $NiCl_2$-treated embryos developed morphologically distinct animal and vegetal boundaries separating it from the larval ectoderm (Fig. 1F). In the treated embryos, pigmentation became regionally distinct as developing pigment cells accumulated in the larval ectoderm in an animal-to-vegetal gradient, leaving vestibular ectoderm relatively unpigmented—exactly as in the untreated embryos (Fig. 1, B–D and F–H). Ciliation disappeared from vestibular ectoderm cells in both treated and untreated embryos.

In normal embryos, a large oval lip formed at the boundary between the outer, larval ectoderm and the inner, vestibular ectoderm, which then constricted in the plane of the lip, reducing the aperture through a medium sized (Fig. 1C) and finally to a very small (Fig. 1D) vestibular opening. Meanwhile, in $NiCl_2$-treated embryos, the two vestibular/larval boundaries (arrowheads in Fig. 1F) also constricted, but in the plane of these boundaries, cutting off the central vestibular region first from the vegetal larval ectoderm, or vegetal lobe (Fig. 1G), and then from the animal larval ectoderm, or animal lobe (Fig. 1H). Finally, as the boundaries constricted, the vestibular ectoderm took on an hourglass shape (Fig. 1H). By this time, the first signs of adult rudiment development (early tube foot primordia) were present in untreated embryos, whereas comparable structures in $NiCl_2$-treated embryos developed about 10 h later.

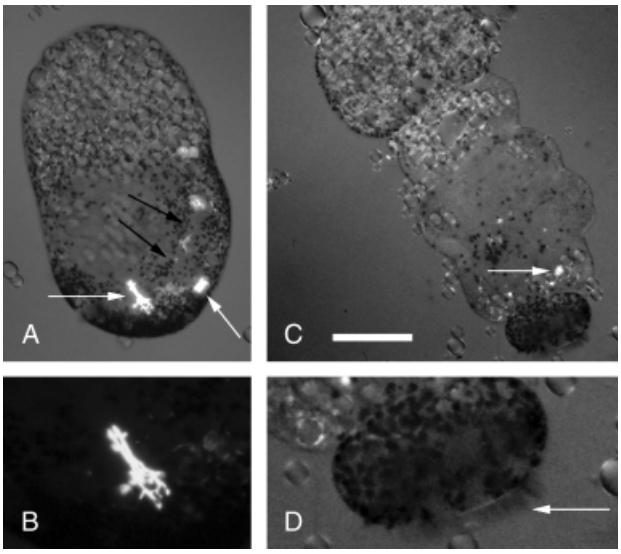

Fig. 2. *Heliocidaris erythrogramma* at 37.5 h viewed under polarized light, which highlights the crystalline $CaCO_3$ skeleton, and also facilitates the visualization of cilia. (A and B) Untreated control viewed from the left side. (A) Larva contains several skeletal elements, at least two of which are larval (white arrows; see Emlet 1995); the others are still too small to score and may be the earliest-forming adult skeleton. The pigment-free stripe can be seen, indicating the path of the ciliated band toward the animal pole (black arrows). (B) Magnified view of larval skeletal rod. (C and D) $NiCl_2$-treated larva. (C) Only a few very small calcite particles are present (arrow), not developed into any larger structures. (D) Magnified view of the ciliated band at the vegetal end of the embryo (arrow). Bar: 200 μm.

The ciliated band formed in normal embryos as early as 30 h, and was indicated earlier, before vestibule closure, by a pigment-free stripe where the ciliated band would later develop (Figs. 1C, D and 2A). The band consists of an open, bilaterally symmetrical loop beginning with two segments along the lateral margins of the vegetal–dorsal surface, parallel to the dorsal midline, which then loop around the vegetal end of the larva along the left and right sides (passing just vegetal to the vestibule on the left side) to meet each other ventrally (Figs. 1D and 2A; and Emlet 1995; Byrne et al. 2001). The band contains long, distinct, densely packed cilia; shorter, sparser cilia remain uniformly distributed over the rest of the larval ectoderm. In $NiCl_2$-treated embryos, the ciliated band was radialized, completely encircling the vegetal pole on the vegetal lobe (Fig. 2, C and D). No band was formed in the vestibular section or in the animal lobe.

At 35–40 h, untreated larvae developed a small, variable number of vestigial larval skeletal rods (Fig. 2, A and B). These rods briefly remained visible until they became obscured by the development of large amounts of adult skeleton at around 45 h. In $NiCl_2$-treated embryos, we did not observe any larval rods (Fig. 2C) at any time up to the delayed appearance of adult skeleton at around 60 h.

At 40–45 h, after continued constriction at the larval/vestibular boundaries, $NiCl_2$-treated larvae stopped spinning around their axes as one unit, and, instead, the central section of vestibular ectoderm became stationary while the animal and vegetal lobes began to spin relative to the central section. Eventually, all of the animal and vegetal lobes detached from the larvae and swam away, continuing to swim without further change for as long as the larvae were cultured, leaving behind the central sections, which did not spin or swim. Development of adult features occurred in the central sections, and was informative about adult axial patterning; this will be described in a separate article (Minsuk et al. unpublished).

H. erythrogramma treated with varying $NiCl_2$ concentrations develop a range of phenotypes

Concentrations of $NiCl_2$ outside the moderate 2–10 μM range caused a wide range of phenotypes, departing from the consistent radialized morphology of the moderately treated embryos.

Above 20 μM, $NiCl_2$ treatment resulted in additional abnormalities. Treatments of 20–100 μM introduced developmental delay (the severity increasing with treatment concentration), as well as additional defects and deformities. Above 100 μM, embryos failed to undergo the normal ectodermal elongation during gastrulation, taking on variable and irregular overall morphologies (not shown). These embryos usually did not form vestibular ectoderm, and never formed adult structures such as tube feet.

At 0.1 μM and below, $NiCl_2$ treatment caused only rare and mild effects. An intermediate concentration, 1.0 μM, caused a spectrum of results within individual cohorts, including normal embryos, completely radialized embryos, and a gradual progression through several intermediate degrees of radialization (Fig. 3). A relatively mild response consisted only of the formation of an abnormally wide vestibular ectodermal territory, still centered on the left side. In the AV direction, this territory was of normal height, but in the DV direction, it covered a wider circumferential arc toward the dorsal and ventral sides of the embryo (Fig. 3A), up to perhaps half of the circumference. The boundary of the territory formed a vestibule lip and was able to close down to a small opening in the usual way, although sometimes forming a dorsoventrally oriented slit.

In more severe responses, the vestibular ectodermal field formed over a substantially larger circumferential arc. In some of these cases, the vestibular ectoderm lacked sharp dorsal and ventral boundaries at all, instead narrowing as it reached around toward the right side, sometimes reaching all the way around but covering less area on the right side than on the left, so that the larval axis could still be discerned (Fig. 3, B and C). Under these conditions, a normal vestibule lip did not form; instead, animal and vegetal lobes pinched off as in fully radialized larvae, although at a pronounced angle reflecting the tapering vestibular–larval boundaries (Fig. 3D). These larvae later formed tube feet on the left side (the widest part of the vestibular ectoderm).

Thus, the radialization does not occur in an all-or-nothing manner, but progressively, with larval left (vestibular ectoderm) expanding at the proportionate expense of larval right (larval ectoderm). Complete radialization (abolishment of the axis altogether, with uniform circumferential differentiation) is only the end point of this progressive axial distortion.

Larvae from this 1.0 μM treatment frequently contained a feature never seen in the higher-concentration treatments. In

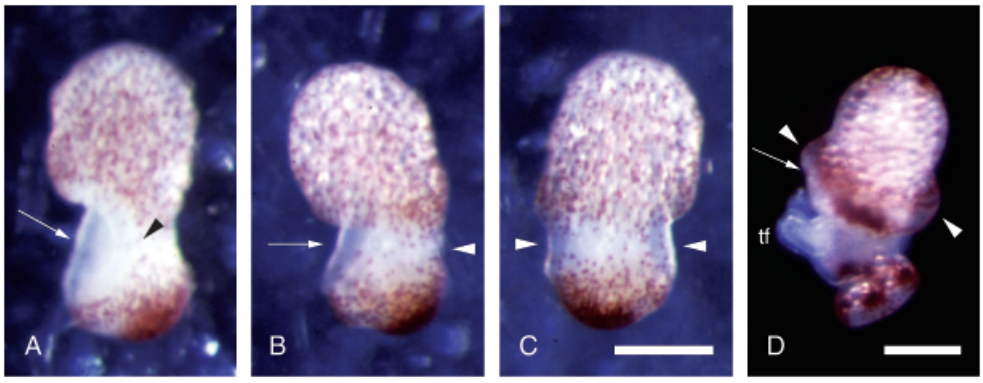

Fig. 3. Intermediate *Heliocidaris erythrogramma* phenotypes in response to reduced $NiCl_2$ dose. (A–C) 29 h. (A) Mild phenotype, in dorsal view. Early vestibule lip reaches abnormally far across the larva toward the right side (arrowhead), causing the vestibule floor to bulge outward (arrow). (B) More severe phenotype, in dorsal view. A tapering vestibular ectoderm reaches around to the right side (arrowhead), and a larger, more distinct and more deeply invaginated region marks the left side (arrow). (C) The same embryo viewed from the right side, showing the narrow but completely circumferential vestibular ectoderm. A slight invagination is visible on the dorsal and ventral sides (arrowheads). (D) Later stage, 43 h, of a larva similar to (B and C), in dorsal view. Animal and vegetal lobes have pinched off, at an angle. Tube feet (tf) have formed in the widest (left side) vestibular region. A second circumferential ciliated band, indicated by its pigment-free stripe (arrow; the cilia themselves cannot be seen in this photo), surrounds the bottom of the animal lobe, supported by a bulging circumferential ridge (arrowheads). Bars: 200 μm.

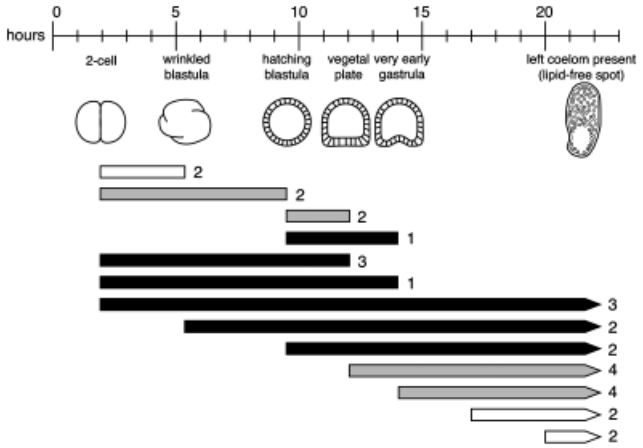

Fig. 4. A range of treatment intervals determines the sensitive period. All experiments were performed with 5 or 10 μM $NiCl_2$. Bars represent treatment period according to the developmental time scale at the top of the figure, and the resulting larval phenotype in each case is indicated by the shading of the bars: black, completely radialized; gray, variable or intermediate; and white, normal. Arrow-tipped bars show treatments that continued through subsequent development. Numbers next to each bar indicate how many experimental cohorts were run under that treatment period. Timing of developmental events is approximate and depends on temperature; treatments were timed according to the morphological mileposts indicated.

addition to a small circumferential ciliated band at the vegetal pole as in the fully radialized larvae, a second, more prominent circumferential ciliated band formed just animal to the vestibular ectoderm (Fig. 3D). These second bands formed without regard to the presence or degree of radialization.

H. erythrogramma is sensitive to $NiCl_2$ between the wrinkled blastula and midgastrula stages, with maximum sensitivity between hatched blastula and vegetal plate formation

In order to characterize the period of sensitivity to $NiCl_2$ (at 5–10 μM), we performed pulsed treatments covering portions of the first day of development (Fig. 4). A completely radialized phenotype as described above was obtained only when the treatment included the period between hatching (lipid-filled coeloblastula from which the earlier wrinkles had disappeared) and vegetal plate formation (Fig. 4, black bars). A pulse covering this period alone did not cause complete radialization, indicating that a longer treatment is required for the full effect.

Treatments ending by the wrinkled blastula stage, or beginning after the midgastrula stage, had no effect (Fig. 4, white bars), indicating the limits of the sensitive period. Treatments covering smaller portions of the interval between these end points produced intermediate or variable phenotypes (Fig. 4, gray bars), comparable with the result described above for reduced $NiCl_2$ concentration throughout development.

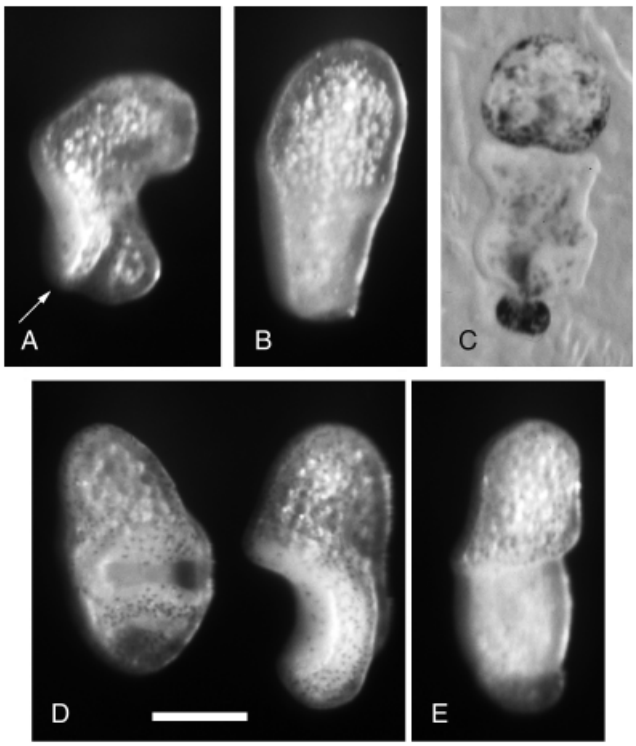

Fig. 5. Surgically altered embryos. (A, B, D, E) are siblings, all at 28 h; slight differences in developmental stage are due to variable degrees of developmental delay routinely caused by surgery (Minsuk and Raff 2002). (A) A cultured ectodermal shell made from an untreated embryo develops normal larval features. Despite the "bent-over" morphology of this specimen (resulting from irregularities in healing after surgery), the animal and vegetal poles were distinguishable by their pigmentation, and the thickened, white, slightly concave vestibular ectoderm can be seen beginning to invaginate on one side of the larva. Arrow: edge of the vestibule lip. (B) An ectodermal shell made from a $NiCl_2$-treated embryo develops radial symmetry, with thickened, circumferential vestibular ectoderm in the vegetal half. (C) An older (44 h) $NiCl_2$-treated ectodermal shell. The fully radialized morphology is evident. (D) Recombinants made by inserting $NiCl_2$-treated archenterons into untreated ectoderm. Vestibules are closing in the normal way. Embryo on the left is in left-side view, looking directly into the shrinking vestibular opening. Embryo on the right is in dorsal view, showing the deep concave vestibular ectoderm on the left side. (E) Recombinant made by inserting an untreated archenteron into a $NiCl_2$-treated ectoderm. The radialized phenotype is unambiguous. Bar: 200 μm.

The effect of $NiCl_2$ on ectodermal patterning is autonomous to the ectoderm

Minsuk and Raff (2002) showed that in untreated embryos after surgical removal of the archenteron (including both endodermal and coelomic precursors) during gastrulation, the resulting ectodermal shell autonomously develops normal larval ectodermal features including the vestibule and ciliated band (Fig. 5A), but fails to develop adult ectodermal features such as tube foot and spine ectoderm or the central nervous

system. These depend upon inductive signals from archenteron derivatives. Recombination of ectoderm and archenteron restores the signal and rescues adult development.

In order to determine whether $NiCl_2$ acts autonomously in the ectoderm, or indirectly through effects on other tissues, we made 23 ectodermal shells from three separate $NiCl_2$-treated spawnings (5–10 μM from the two-cell stage until surgery). The critical period of $NiCl_2$ sensitivity has already passed by the time surgery is performed at the gastrula stage. All $NiCl_2$-treated ectodermal shells developed a radialized ectodermal morphology identical to that of intact $NiCl_2$-treated embryos (Fig. 5, B and C). Radialization therefore does not depend on the presence of the endoderm or coelomic mesoderm after the gastrula stage.

To further test this question, we removed and exchanged archenterons between treated and untreated embryos, producing 22 reciprocal ectoderm/archenteron recombinants. Two specimens healed too poorly to score and were discarded. The remainder developed entirely according to the treatment of the ectoderm. Seven recombinants containing untreated ectoderm all developed normally patterned larvae with well-formed vestibules; the presence of $NiCl_2$-treated endoderm and coelomic mesoderm had no effect on ectodermal development (Fig. 5D). Likewise, recombinants containing $NiCl_2$-treated ectoderm (13 from two separate spawnings) all developed radialized larvae; axial patterning was not rescued by the presence of normal endoderm and coelomic mesoderm (Fig. 5E).

Ectodermal shells and archenteron explants both carry significant amounts of mesenchyme (Minsuk and Raff 2002). Therefore, we cannot definitively rule out an influence of treated mesenchyme cells on ectoderm. However, the mixture of treated and untreated mesenchyme in reciprocal recombinants neither rescues treated ectoderm from radialization, nor causes radialization in untreated ectoderm. It therefore appears that mesenchyme, like endoderm and coelom, is not involved in the response of ectoderm to $NiCl_2$. Therefore, larval ectodermal axial patterning is autonomous, consistent with the other aspects of autonomous larval ectoderm development shown previously (Minsuk and Raff 2002), and $NiCl_2$ disrupts this patterning process by acting directly on the ectoderm.

DISCUSSION

$NiCl_2$ radializes *H. erythrogramma*, suggesting conserved mechanisms of axis determination

Williams and Anderson (1975) described an alternative larval morph of *H. erythrogramma*, later determined to be a pathology, in which the vestibule develops abnormally; tube feet and spines develop externally, but a viable juvenile does not form. This phenotype occurs spontaneously in overcrowded or warm cultures (our unpublished observations). We hypothesized that this phenotype represents a specific patterning defect in which all ectodermal cells acquire a left-side identity, resulting in a radialized larva. By analogy with the radialization of *L. variegatus* (Hardin et al. 1992), we predicted that $NiCl_2$ treatment would duplicate this phenotype. Indeed, $NiCl_2$ treatment produced a radially symmetric *H. erythrogramma* larval phenotype (Fig. 1, E–H) exactly duplicating that seen by Williams and Anderson (1975). Treated embryos gastrulated normally, but then formed a vestibular ectoderm along a circumferential band. The response was ectoderm autonomous, and showed a progressive, concentration-dependent shift of territory boundaries. The larval cells and tissues remained healthy and went on to produce adult structures.

To establish a baseline for the genus *Heliocidaris*, we tested *H. tuberculata*, the indirect-developing sister species of *H. erythrogramma*. This species exhibits the same radialized phenotype in response to $NiCl_2$ as *L. variegatus* (Hardin et al. 1992), *L. pictus* (Timourian and Watchmaker 1972), *Dendraster excentricus* (Rulon 1953), and *Paracentrotus lividus* (Lallier 1956; Di Bernardo et al. 1999; Duboc et al. 2004).

The response of *H. erythrogramma* to $NiCl_2$ treatment shares many similarities with that of indirect developers. All the features listed in Table 1 have been documented in $NiCl_2$-treated *L. variegatus* (Hardin et al. 1992; Armstrong et al. 1993). This consistent suite of phenotypic characteristics constitutes a recognizable syndrome of developmental response, strongly suggesting action via a single homologous pathway (or set of pathways responding to a single sensitive upstream regulatory control). These species have been diverging for 200 Myr (Smith 1984), demonstrating strong conservation of the nickel-sensitive pathway and its role in axial patterning. *H. tuberculata* and *H. erythrogramma* are only 4 million years apart (Zigler et al. 2003), so nickel most likely interferes with a homologous molecular pathway in *H. erythrogramma*. If it does, then such a syndrome of responses (Table 1) would be expected. We consider the alternatives highly unlikely: that the complete syndrome in *H. erythrogramma*, in response to the same experimental treatment, arises coincidentally and convergently via an unrelated pathway, or via nonspecific physiological disruption.

The paradox of sinistralization

Despite the similarities between the radialization of *H. erythrogramma* and other sea urchins, there is one important difference. In indirect developers, including *H. tuberculata*, nickel causes ventralization (Hardin et al. 1992): the progressive expansion of a ventral tissue type (oral ectoderm) at the expense of a dorsal one (aboral ectoderm). In *H. erythrogramma*, it causes sinistralization: expansion of a left-side tissue type (vestibular ectoderm) at the expense of a right-side one (larval ectoderm). *H. erythrogramma* also differs with respect to skeleton formation (Table 1), but this is probably secondary to the difference in ectodermal patterning, as discussed in a later section.

Table 1. Response to $NiCl_2$ treatment: *Heliocidaris erythrogramma* versus indirect developers

Similarities	Differences
Radially symmetrical ectoderm	Sinistralization in *H. erythrogramma* (expansion of vestibular ectoderm, a left-side tissue type, at the expense of larval ectoderm), versus ventralization in indirect developers (expansion of oral at the expense of aboral ectoderm)
Concentration-dependent response, with intermediate phenotypes showing a gradual shift of territory boundaries, until at maximum response only a single territory is expressed	
Similar $NiCl_2$-sensitive period (wrinkled blastula to midgastrula in *H. erythrogramma*; hatched blastula to early gastrula in *L. variegatus*)	Elimination of larval skeleton in *H. erythrogramma* versus proliferation in indirect developers
After fully radializing doses, a single circumferential ciliated band restricted to the vegetal pole	
After intermediate doses, a second circumferential ciliated band near the animal pole	
Ectoderm-autonomous response	

H. erythrogramma has a distinct larval bilateral symmetry inherited from its indirect-developing ancestors, with ventral and dorsal midlines indicated by the remnant larval characters, the ciliated band and the vestigial larval skeleton (Emlet 1995; Byrne et al. 2001), and reflected in transient, remnant DV patterning of *goosecoid* (*Gsc*) gene expression in the early gastrula (Wilson et al. 2005a). Relative to these landmarks, the vestibule is distinctly restricted to the left side. Its expansion is not ventralization, which would shift all cells toward a more ventral fate (Hardin et al. 1992); instead, it requires ventral midline cells to form vestibule, normally found only more dorsally and further left. No ventralized phenotype has ever been identified in *H. erythrogramma*.

The similarities between the broadly conserved specific $NiCl_2$ sensitivity of other echinoids and that of *H. erythrogramma* suggest a fundamental homology, but the ventralization/sinistralization discrepancy poses an apparent paradox. The explanation must reside in the nature of larval axis determination, and in the mechanism by which nickel interferes with this process. We next consider these two issues in turn.

Axis formation in indirect and direct development

The larval axes in indirect developers arise progressively (reviewed in Henry 1998; Brandhorst and Klein 2002; Angerer and Angerer 2003). Maternal AV patterning, and events during early cleavage stages along the DV and LR axes, specify the locations and polarity of the axes but not the regional identities and specific tissue types that differentiate along each one. These are determined only later, by a series of cell–cell inductive interactions that set up regional gene expression territories (McCain and McClay 1994; Kirchhamer and Davidson 1996; Summers et al. 1996; Wikramanayake and Klein 1997; Henry 1998; Angerer et al. 2001; Coffman and Davidson 2001; Duboc et al. 2004; Wilson et al. 2005a,b). Along the DV axis, knockdown or overexpression of dorsally or ventrally restricted genes such as *Gsc*, *Otx*, or *nodal* (Angerer et al. 2001; Duboc et al. 2004), as well as nickel or other treatments (Hardin et al. 1992; Coffman and Davidson 2001), can disrupt differentiation of oral and aboral fates until the gastrula stage, when they finally become committed. The LR axis becomes committed around the same time (McCain and McClay 1994; Summers et al. 1996; Henry 1998).

H. erythrogramma larvae develop a different morphology. They have a distinct DV axis and bilateral symmetry, but no mouth or oral/aboral boundary; the ciliated band (which separates those territories in indirect developers) is open-ended, within a homogeneous larval ectoderm (Emlet 1995; Haag and Raff 1998; Raff and Sly 2000; Byrne et al. 2001; Love and Raff unpublished). Nonetheless, axis formation follows a generally similar scheme (Kauffman and Raff 2003; Wilson et al. 2005a,b). The LR axis is established before first cleavage, but cell fates along this axis are not fully committed until at least gastrulation (Henry and Raff 1990, 1994; Henry et al. 1990; Minsuk et al. 2005). Hybridization of *H. erythrogramma* eggs and *H. tuberculata* sperm illustrates the compatibility of basic axis formation mechanisms (Raff et al. 1999). These hybrids support the development of all three embryonic axes, and a distinct oral field containing a mouth, separated from the aboral field by a closed ciliated band. Notably, the vestibular ectoderm forms later, in a small patch of ectoderm just to the left of the mouth and well within the oral field, just as in indirect developers.

In indirect developers, nickel perturbs the pathway by which tissues along the already specified DV axis commit to oral and aboral fates (Hardin et al. 1992; Di Bernardo et al. 1999; Duboc et al. 2004), probably acting at the same point in the pathway in all indirect developers. The similarities in *H. erythrogramma* axis formation suggest that nickel should interfere with axis determination via a similar mechanism in this species.

Mechanisms of action of nickel

Nickel can have general physiological effects by, for example, interfering with Na^+ or Ca^{2+} channels (Zamponi et al. 1996;

Cucu et al. 2003; Sheng et al. 2004), which may explain the severe defects caused by the highest $NiCl_2$ concentrations in both *Heliocidaris* species as well as in *L. variegatus* (Hardin et al. 1992). But at moderate doses, $NiCl_2$ causes a controlled transformation of cell fates by modifying gene expression patterns (Hardin et al. 1992; Di Bernardo et al. 1999; Duboc et al. 2004), and recent studies have shown a variety of mechanisms by which such specific effects can occur (Kasprzak et al. 2003). Nickel-induced Ca^{2+} elevation can itself lead to quite selective gene activation (Salnikow et al. 2002). Nickel can also act directly on gene regulation, for example by interfering with the zinc-binding site of zinc finger transcription factors, altering their DNA-binding affinity or sequence specificity (Nagaoka et al. 1993; Hartwig 2001). Of particular interest is the ability of nickel to interfere with the mammalian hypoxia response pathway (Semenza 2001; Hewitson et al. 2003). Transcription of hypoxia response genes is triggered by the master switch HIF-1α, regulated by several iron-dependent hydroxylases that directly sense O_2. Under normoxia, post-translational hydroxylation suppresses HIF-1α. Hypoxia deactivates the hydroxylases, activating HIF-1α and downstream transcription. Ni^{2+} ions mimic the hypoxic trigger, leading to inappropriate activation of the pathway, and to cancer (Salnikow et al. 2000; Kasprzak et al. 2003). The pathway is also important in early development (Iyer et al. 1998; Ryan et al. 1998; Lavista-Llanos et al. 2002; Nishi et al. 2004). Sea urchin homologues of HIF-1α and the HIF hydroxylases have not yet been identified, but the connection between an oxygen-sensing pathway and the ability of nickel to interfere with transcriptional regulation is highly suggestive in light of a study by Coffman and Davidson (2001), showing that in sea urchins, an imposed redox gradient biases the DV axis, entraining oral differentiation at the high end of the gradient. The HIF-1α pathway and its O_2-sensing role are conserved in *Caenorhabditis* and *Drosophila* (Epstein et al. 2001; Lavista-Llanos et al. 2002). The same pathway in sea urchins could mediate normal oral/aboral patterning, axis entrainment by redox gradients, and radialization by nickel; in *H. erythrogramma*, modified regulation of this pathway could have resulted in the evolution of vestibular patterning as discussed below.

We do not know the particular chemical mechanism by which nickel interferes with axial patterning. But its various known effects make it clear that nickel has the capacity for specific modification of gene expression, consistent with the phenotypic evidence discussed earlier. We know that nickel acts early in the process, after the initial specification of the axes, but upstream of all known players in the subsequent progressive determination of region-specific cell types along the axes (Hardin et al. 1992; Di Bernardo et al. 1999; Duboc et al. 2004). Based on these facts, we propose the following model.

Co-option from DV to LR axial patterning during the evolution of direct development in *H. erythrogramma*

In indirect developers, the conserved nickel-sensitive pathway patterns oral and aboral ectoderm along the DV axis; in *H. erythrogramma*, it may have been redeployed to pattern vestibular and larval ectoderm along the LR axis. This may not require a major evolutionary rewiring. A differentiated oral ectoderm is absent in *H. erythrogramma*, and the vestibule may represent its sole morphological remnant, as it is clearly homologous to the vestibules of indirect developers, which are orally derived. In indirect developers, oral ectodermal features are patterned by short-range signals within the oral territory (Hardin and Armstrong 1997; Di Bernardo et al. 1999); if vestibular fate is controlled by similar signals, then it would depend upon oral differentiation and hence upon DV patterning. As noted above, vestibule development follows the typical indirect-developing pattern in *H. erythrogramma* × *H. tuberculata* hybrids (Raff et al. 1999). It appears that once oral/aboral patterning has been reconstituted in the hybrid embryo, vestibule development naturally comes under its control. This suggests that the *H. erythrogramma* vestibule represents an orphaned sub-module that remained when the parent module of oral development was lost.

How, then, could this differentiation pathway have become redeployed along the LR axis? Vestibular fate in indirect developers must be regulated not only by DV but also by LR signals, because the vestibule arises asymmetrically, to the left of the mouth. We hypothesize that when the oral territory was lost from the *H. erythrogramma* lineage, the controls imposed by oral ectoderm on vestibular development were concomitantly lost, allowing the vestibular territory to develop solely under the control of LR signals. At the level of axial patterning, this is seen as a co-option of the nickel-sensitive pathway from DV to LR axis regulation, with the attendant transformation of the nickel-induced phenotype. At the level of tissue-type differentiation, it may be fundamentally conservative. In indirect developers, the pathway regulates the boundary of the oral ectoderm. If *H. erythrogramma* vestibular ectoderm is the remnant of the oral ectoderm, then a radical shift in axial orientation may have occurred by the loss of one upstream regulatory control with no change in target function.

Recent studies of *Gsc* gene expression and function in *Heliocidaris* support this interpretation. *Gsc* is expressed in the oral ectoderm in *H. tuberculata* as in other indirect developers (Wilson et al. 2005a), and is radialized by $NiCl_2$ treatment (Duboc et al. 2004), indicating that it acts downstream of the point where $NiCl_2$ acts on DV patterning. In *H. erythrogramma*, *Gsc* retains a transient ventral expression pattern in the gastrula, but quickly downregulates in most of the territory and becomes concentrated in the developing vestibular ectoderm (Wilson et al. 2005a), suggesting that *Gsc*

has become co-opted into a role in vestibule development. Overexpression restores some features of the oral ectoderm, whereas knockout has no detectable effect on development, suggesting that an ancestral DV patterning role has been lost (Wilson et al. 2005b). If a nickel-sensitive pathway in DV axial patterning has been co-opted into LR axis regulation, this is just the kind of behavior we would predict for genes downstream in that pathway.

The failure of the vestigial larval skeleton to form in treated *H. erythrogramma* embryos is consistent with this model, and with an ectodermal role in patterning the limited larval skeleton. Because oral ectoderm in indirect developers patterns larval skeleton, the expansion of oral territory in nickel-treated embryos leads to a proliferation of circumferentially distributed triradiate spicules. In contrast, *H. erythrogramma* lacks oral ectoderm, and the expansion of vestibular territory in nickel-treated embryos leads to a loss of larval skeleton (even though the mesenchyme is competent to produce adult skeleton; Minsuk et al. unpublished). This suggests that mesenchyme cells may normally receive skeleton-inducing signals from the larval ectoderm, and/or inhibitory signals from the vestibular ectoderm. The evolutionary reduction in larval skeletal elements in normal embryos and their variability in size and number (Emlet 1995, and our unpublished observations) may be directly linked to the loss of the oral ectoderm gene expression module (Zhou et al. 2003; Wilson et al. 2005a,b). If the larval skeleton is indeed patterned by the ectoderm in *H. erythrogramma*, it would support our prediction (Minsuk and Raff 2002) that the coelom-dependent patterning of adult skeleton represents a difference between larval and adult skeletal patterning in sea urchins generally, rather than a peculiarity of *H. erythrogramma*.

Sinistralization and morphogenesis: convergent extension of the vestibule lip

The unusual morphogenesis of nickel-treated *H. erythrogramma* embryos further supports our interpretation of this phenotype as a global expression of left-side identity. In normal embryos, the vestibular ectodermal field invaginates to form an internal cavity; its initially wide perimeter (the vestibular–larval boundary) becomes a distinct vestibule lip that shrinks dramatically (Figs. 1A–D and 6A; and Ferkowicz and Raff 2001). This tissue undergoes enormous topological distortion as the opening shrinks, constituting a circumferential convergence coupled to a radial extension—an important class of morphogenetic transformation among metazoan taxa (Keller 1987; Keller et al. 2000). The mechanism by which this is accomplished at the level of the individual cells has not been studied, but is likely to involve extensive cell rearrangement, possibly in combination with cell shape changes or other anisotropic processes (Keller 1987; Weliky et al. 1991; Keller et al. 2000). These are likely to be active, force-generating processes because the vestibule lip is relatively isolated from other tissues. (It is surrounded mostly by sea water; see Fig. 6A.) The amount of distortion, and therefore of cellular morphogenetic activity, must be greatest near the lip, and decrease with increasing distance from the lip on both sides of the boundary. Therefore, the boundary region exhibits specialized behavior. As a left-side identity progressively expands toward the right side, ending in complete sinistralization (Fig. 6B), the boundary cells would be deployed around an increasingly wide vestibular field that finally encircles the embryo completely, resulting in two vestibular–larval boundaries separating the vestibular ectoderm from the animal and vegetal lobes. If the combined individual cell behaviors along

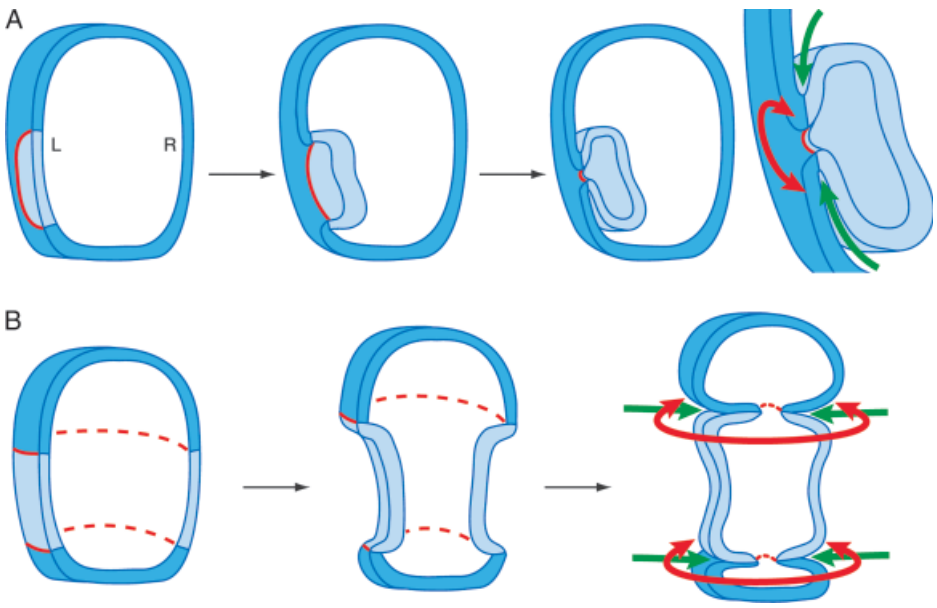

Fig. 6. (A) Normal vestibule formation and closure, showing the ectoderm only; endoderm and mesoderm have been omitted. L, left side of embryo; R, right side. Larval ectoderm is in darker blue, vestibular ectoderm in light blue. Vestibular–larval boundary outlined in red. The vestibule begins as a patch of ectoderm on the left side. As the vestibule invaginates, the boundary shrinks, displaying circumferential convergence, parallel to the boundary (red arrow in the magnified final panel), and radial extension, perpendicular to the boundary (green arrows). (B) A sinistralized vestibule field encircles the embryo, resulting in two separate boundaries. Normal local behavior at the boundaries as described in (A) predicts the observed morphogenesis: circumferential convergence and radial extension cause the boundaries to constrict.

Table 2. Dosage sensitivity to $NiCl_2$ treatment (concentrations in μM) in various echinoids

Species	Partial radialization	Full radialization	Additional defects
Dendraster excentricus (Rulon 1953)		300	1250
Paracentrotus lividus (Lallier 1956)	40	80	≥ 400
P. lividus (Di Bernardo et al. 1999; Duboc et al. 2004)		500	
Lytechinus pictus (Timourian and Watchmaker 1972)		1–100[1]	≥ 1000
L. variegatus (Hardin et al. 1992)	100–250	500–1000	>2000
Hemicentrotus pulcherrimus (N. Tokuoka personal communication)		100–1000	>1000
Heliocidaris tuberculata (this study)	5	50	500
H. erythrogramma (this study)	1	2–10	≥ 100

[1]Timourian and Watchmaker (1972) did not report any one treatment level that resulted consistently in full radialization; they observed a range of phenotypes evidently including fully radialized embryos, along with both partially radialized and hyperdefective (nongastrulating) embryos, at 1, 10, and 100 μM.

these ectopic boundaries can still produce their normal collective convergence (parallel to the boundary) and extension (perpendicular to the boundary), the net result would be exactly what is seen in sinistralized embryos: the constriction of the two boundaries resulting in the separation of the two lobes (Fig. 6B). In intermediate cases, vestibular invagination fails and is transformed into constriction if a critical level of sinistralization is reached (Fig. 3).

Sinistralization also explains the spinning and detachment of the animal and vegetal lobes. Embryos spin because of their uniform ciliation, which is lost in the vestibular ectoderm. In sinistralized embryos, only the two lobes are ciliated, so they spin independently and eventually twist off. Thus, the abnormal morphogenesis of radialized embryos is entirely explicable in light of the ectopic circumferential redeployment of otherwise normal vestibular ectoderm and vestibular–larval boundary cells.

Increased sensitivity to radialization in *H. erythrogramma*

Sensitivity to nickel varies among echinoids, as shown in Table 2, and the genus *Heliocidaris* is particularly sensitive. *H. tuberculata* is at least 10 times more sensitive than *L. variegatus*, and *H. erythrogramma* is approximately 10 times more sensitive than *H. tuberculata*. It is important to take these differences into account during experiments; the dosage appropriate for *L. variegatus* is not necessarily appropriate for other species (Table 2), and may cause unwanted defects that could complicate the interpretation of results.

Given the available data, we cannot determine whether these differences are related to developmental mode, to phylogenetic divergence, or to a combination of both, with increased sensitivity in the genus *Heliocidaris* possibly having some impact on the evolution of direct development in *H. erythrogramma*. The evolution of direct development has involved the modification of other quantitative features of development, such as oocyte growth regulation (Byrne et al. 1999) and the timing of axis specification (Henry and Raff 1990; Henry et al. 1990). The sensitivity of *H. erythrogramma* to radialization (by $NiCl_2$, heat, or overcrowding) indicates a reduction of buffering against environmental effects. The demonstration that an environmental parameter (O_2 concentration) regulates development in many taxa (Iyer et al. 1998; Ryan et al. 1998; Coffman and Davidson 2001; Lavista-Llanos et al. 2002; Nishi et al. 2004) opens the possibility that such sensitivity could arise as a side-effect of an adaptation.

Acknowledgments

We thank the Sydney Aquarium and the School of Biological Sciences, University of Sydney for providing resources, and for making our work in Australia possible. In particular, Malcolm Rickett provided invaluable assistance with microscopy and photography. Thanks also to Gerd Müller for comments on the manuscript. New South Wales Fisheries provided permits for collecting sea urchins. This work was funded by an NIH Postdoctoral Fellowship to S. B. M. and an NSF research grant to R. A. R.

REFERENCES

Angerer, L. M., and Angerer, R. C. 2003. Patterning the sea urchin embryo: gene regulatory networks, signaling pathways, and cellular interactions. *Curr. Top. Dev. Biol.* 53: 159–198.

Angerer, L. M., Oleksyn, D. W., Levine, A. M., Li, X., Klein, W. H., and Angerer, R. C. 2001. Sea urchin goosecoid function links fate specification along the animal–vegetal and oral–aboral embryonic axes. *Development* 128: 4393–4404.

Armstrong, N., Hardin, J., and McClay, D. R. 1993. Cell–cell interactions regulate skeleton formation in the sea urchin embryo. *Development* 119: 833–840.

Brandhorst, B. P., and Klein, W. H. 2002. Molecular patterning along the sea urchin animal–vegetal axis. *Int. Rev. Cytol.* 213: 183–232.

Byrne, M., Emlet, R. B., and Cerra, A. 2001. Ciliated band structure in planktotrophic and lecithotrophic larvae of *Heliocidaris* species (Echinodermata: Echinoidea): a demonstration of conservation and change. *Acta Zool.* 82: 189–199.

Byrne, M., Villinski, J. T., Cisternas, P., Siegel, R. K., Popodi, E., and Raff, R. A. 1999. Maternal factors and the evolution of developmental mode: evolution of oogenesis in *Heliocidaris erythrogramma*. *Dev. Genes Evol.* 209: 275–283.

Coffman, J. A., and Davidson, E. H. 2001. Oral–aboral axis specification in the sea urchin embryo I. Axis entrainment by respiratory asymmetry. *Dev. Biol.* 230: 18–28.

Cucu, D., Simaels, J., Van Driessche, W., and Zeiske, W. 2003. External Ni^{2+} and ENaC in A6 cells: Na^+ current stimulation by competition at a binding site for amiloride and Na^+. *J. Membrane Biol.* 194: 33–45.

Di Bernardo, M., et al. 1999. Spatially restricted expression of *PlOtp*, a *Paracentrotus lividus Orthopedia*-related homeobox gene, is correlated with oral ectodermal patterning and skeletal morphogenesis in late-cleavage sea urchin embryos. *Development* 126: 2171–2179.

Duboc, V., Röttinger, E., Besnardeau, L., and Lepage, T. 2004. Nodal and BMP2/4 signaling organizes the oral–aboral axis of the sea urchin embryo. *Dev. Cell* 6: 397–410.

Emlet, R. B. 1995. Larval spicules, cilia, and symmetry as remnants of indirect development in the direct developing sea urchin *Heliocidaris erythrogramma*. *Dev. Biol.* 167: 405–415.

Epstein, A. C. R., et al. 2001. *C. elegans* EGL-9 and mammalian homologs define a family of dioxygenases that regulate HIF by prolyl hydroxylation. *Cell* 107: 43–54.

Ferkowicz, M. J., and Raff, R. A. 2001. Wnt gene expression in sea urchin development: heterochronies associated with the evolution of developmental mode. *Evol. Dev.* 3: 24–33.

Finnerty, J. R., Pang, K., Burton, P., Paulson, D., and Martindale, M. Q. 2004. Origins of bilateral symmetry: *Hox* and *Dpp* expression in a sea anemone. *Science* 304: 1335–1337.

Gerhart, J. 2000. Inversion of the chordate body axis: are there alternatives? *Proc. Natl. Acad. Sci. USA* 97: 4445–4448.

Haag, E. S., and Raff, R. A. 1998. Isolation and characterization of three mRNAs enriched in embryos of the direct-developing sea urchin *Heliocidaris erythrogramma*: evolution of larval ectoderm. *Dev. Genes Evol.* 208: 188–204.

Hardin, J., and Armstrong, N. 1997. Short-range cell–cell signals control ectodermal patterning in the oral region of the sea urchin embryo. *Dev. Biol.* 182: 134–149.

Hardin, J., Coffman, J. A., Black, S. D., and McClay, D. R. 1992. Commitment along the dorsoventral axis of the sea urchin embryo is altered in response to $NiCl_2$. *Development* 116: 671–685.

Hartwig, A. 2001. Zinc finger proteins as potential targets for toxic metal ions: differential effects on structure and function. *Antioxid. Redox Signal.* 3: 625–634.

Henry, J. J. 1998. The development of dorsoventral and bilateral axial properties in sea urchin embryos. *Sem. Cell Devel. Biol.* 9: 43–52.

Henry, J. J., and Raff, R. A. 1990. Evolutionary change in the process of dorsoventral axis determination in the direct developing sea urchin, *Heliocidaris erythrogramma*. *Dev. Biol.* 141: 55–69.

Henry, J. J., and Raff, R. A. 1994. Progressive determination of cell fates along the dorsoventral axis in the sea urchin *Heliocidaris erythrogramma*. *Rouxs Arch. Dev. Biol.* 204: 62–69.

Henry, J. J., Wray, G. A., and Raff, R. A. 1990. The dorsoventral axis is specified prior to first cleavage in the direct developing sea urchin *Heliocidaris erythrogramma*. *Development* 110: 875–884.

Henry, J. J., Wray, G. A., and Raff, R. A. 1991. Mechanism of an alternate type of echinoderm blastula formation: the wrinkled blastula of the sea urchin *Heliocidaris erythrogramma*. *Dev. Growth Differ.* 33: 317–328.

Hewitson, K. S., McNeill, L. A., Elkins, J. M., and Schofield, C. J. 2003. The role of iron and 2-oxoglutarate oxygenases in signalling. *Biochem. Soc. Trans.* 31: 510–515.

Hörstadius, S. 1973. *Experimental Embryology of Echinoderms*. Clarendon Press, Oxford.

Iyer, N. V., et al. 1998. Cellular and developmental control of O_2 homeostasis by hypoxia-inducible factor 1α. *Genes Dev.* 12: 149–162.

Kasprzak, K. S., Sunderman, F. W. Jr., and Salnikow, K. 2003. Nickel carcinogenesis. *Mutat. Res.* 533: 67–97.

Kauffman, J. S., and Raff, R. A. 2003. Patterning mechanisms in the evolution of derived developmental life histories: the role of Wnt signaling in axis formation of the direct-developing sea urchin *Heliocidaris erythrogramma*. *Dev. Genes Evol.* 213: 612–624.

Keller, R. 1987. Cell rearrangement in morphogenesis. *Zool. Sci.* 4: 763–779.

Keller, R., et al. 2000. Mechanisms of convergence and extension by cell intercalation. *Philos. Trans. R. Soc. Lond. B.* 355: 897–922.

Kirchhamer, C. V., and Davidson, E. H. 1996. Spatial and temporal information processing in the sea urchin embryo: modular and intramodular organization of the *CyIIIa* gene *cis*-regulatory system. *Development* 122: 333–348.

Lallier, R. 1956. Les ions de métaux lourds et le problème de la détermination embryonnaire chez les échinodermes. *J. Embryol. Exp. Morphol.* 4: 265–278.

Lavista-Llanos, S., et al. 2002. Control of the hypoxic response in *Drosophila melanogaster* by the basic helix–loop–helix PAS protein Similar. *Mol. Cell. Biol.* 22: 6842–6853.

McCain, E. R., and McClay, D. R. 1994. The establishment of bilateral asymmetry in sea urchin embryos. *Development* 120: 395–404.

Minsuk, S. B., Andrews, M. E., and Raff, R. A. 2005. From larval bodies to adult body plans: patterning the development of the presumptive adult ectoderm in the sea urchin larva. *Dev. Genes Evol.* (in press).

Minsuk, S. B., and Raff, R. A. 2002. Pattern formation in a pentameral animal: induction of early adult rudiment development in sea urchins. *Dev. Biol.* 247: 335–350.

Nagaoka, M., Kuwahara, J., and Sugiura, Y. 1993. Alteration of DNA binding specificity by nickel (II) substitution in three zinc (II) fingers of transcription factor Sp1. *Biochem. Biophys. Res. Commun.* 194: 1515–1520.

Nishi, H., et al. 2004. Hypoxia-inducible factor-1 transactivates transforming growth factor-β3 in trophoblast. *Endocrinology* 145: 4113–4118.

Popodi, E., and Raff, R. A. 2001. Hox genes in a pentameral animal. *BioEssays* 23: 211–214.

Raff, E. C., Popodi, E. M., Sly, B. J., Turner, F. R., Villinski, J. T., and Raff, R. A. 1999. A novel ontogenetic pathway in hybrid embryos between species with different modes of development. *Development* 126: 1937–1945.

Raff, R. A. 1987. Constraint, flexibility, and phylogenetic history in the evolution of direct development in sea urchins. *Dev. Biol.* 119: 6–19.

Raff, R. A., and Sly, B. J. 2000. Modularity and dissociation in the evolution of gene expression territories in development. *Evol. Dev.* 2: 102–113.

Rulon, O. 1953. The modification of developmental patterns in the sand dollar with nickelous chloride. *Anat. Rec.* 117: 615.

Ryan, H. E., Lo, J., and Johnson, R. S. 1998. HIF-1α is required for solid tumor formation and embryonic vascularization. *EMBO J.* 17: 3005–3015.

Salnikow, K., Blagosklonny, M. V., Ryan, H., Johnson, R., and Costa, M. 2000. Carcinogenic nickel induces genes involved with hypoxic stress. *Cancer Res.* 60: 38–41.

Salnikow, K., et al. 2002. The regulation of hypoxic genes by calcium involves c-Jun/AP-1, which cooperates with the hypoxia-inducible factor 1 in response to hypoxia. *Mol. Cell. Biol.* 22: 1734–1741.

Semenza, G. L. 2001. HIF-1, O_2, and the 3 PHDs: how animal cells signal hypoxia to the nucleus. *Cell* 107: 1–3.

Sheng, S., Perry, C. J., and Kleyman, T. R. 2004. Extracellular Zn^{2+} activates epithelial Na^+ channels by eliminating Na^+ self-inhibition. *J. Biol. Chem.* 279: 31687–31696.

Smith, A. 1984. *Echinoid Paleobiology*. Allen & Unwin, London.

Summers, R. G., Piston, D. W., Harris, K. M., and Morrill, J. B. 1996. The orientation of first cleavage in the sea urchin embryo, *Lytechinus variegatus*, does not specify the axes of bilateral symmetry. *Dev. Biol.* 175: 177–183.

Timourian, H., and Watchmaker, G. 1972. Nickel uptake by sea urchin embryos and their subsequent development. *J. Exp. Zool.* 182: 379–388.

Weliky, M., Minsuk, S., Keller, R., and Oster, G. 1991. Notochord morphogenesis in *Xenopus laevis*: simulation of cell behavior underlying tissue convergence and extension. *Development* 113: 1231–1244.

Wikramanayake, A. H., and Klein, W. H. 1997. Multiple signaling events specify ectoderm and pattern the oral–aboral axis in the sea urchin embryo. *Development* 124: 13–20.

Williams, D. H. C., and Anderson, D. T. 1975. The reproductive system, embryonic development, larval development and metamorphosis of the sea urchin *Heliocidaris erythrogramma* (Val.) (Echinoidea: Echinometridae). *Aust. J. Zool.* 23: 371–403.

Wilson, K. A., Andrews, M. E., and Raff, R. A. 2005a. Dissociation of expression patterns of homeodomain transcription factors in the evolution of developmental mode in the sea urchins *Heliocidaris tuberculata* and *H. erythrogramma*. *Evol. Dev.* (in press).

Wilson, K. A., Andrews, M. E., Turner, F. R., and Raff, R. A. 2005b. Major regulatory factors in the evolution of development: the roles of *goosecoid* and *Msx* in the evolution of the direct-developing sea urchin *Heliocidaris erythrogramma*. *Evol. Dev.* (in press).

Wray, G. A., and Raff, R. A. 1989. Evolutionary modification of cell lineage in the direct-developing sea urchin *Heliocidaris erythrogramma*. *Dev. Biol.* 132: 458–470.

Wray, G. A., and Raff, R. A. 1990. Novel origins of lineage founder cells in the direct-developing sea urchin *Heliocidaris erythrogramma*. *Dev. Biol.* 141: 41–54.

Zamponi, G. W., Bourinet, E., and Snutch, T. P. 1996. Nickel block of a family of neuronal calcium channels: subtype- and subunit-dependent action at multiple sites. *J. Membrane Biol.* 151: 77–90.

Zhou, N., Wilson, K. A., Andrews, M. E., Kauffman, J. S., and Raff, R. A. 2003. Evolution of OTP-independent larval skeleton patterning in the direct-developing sea urchin, *Heliocidaris erythrogramma*. *J. Exp. Zool. Part B. Mol. Dev. Evol.* 300B: 58–71.

Zigler, K. S., Raff, E. C., Popodi, E., Raff, R. A., and Lessios, H. A. 2003. Adaptive evolution of bindin in the genus *Heliocidaris* is correlated with the shift to direct development. *Evolution* 57: 2293–3202.